

QUASIOPTICAL PHONON-COOLED NbN

HOT-ELECTRON BOLOMETER MIXER AT THz FREQUENCIES

P.Yagoubov, G.Gol'tsman, B.Voronov, S.Svechnikov, S.Cherednichenko, and E.Gershenson
Department of Physics, Moscow State Pedagogical University, Moscow 119435, Russia

V.Belitsky, H.Ekström, and E.Kollberg
Chalmers University of Technology, S-412 96, Göteborg, Sweden

A.Semenov, Yu.Gousev, and K.Renk
Institute of Applied Physics, University of Regensburg, 93040 Regensburg, Germany

Abstract

In our experiments we tested phonon-cooled hot-electron bolometer (HEB) quasioptical mixer based on spiral antenna designed for 0.5-1.2 THz frequency band and fabricated on sapphire, Si-coated sapphire and high resistivity silicon substrates. HEB devices were produced from thin superconducting NbN film 3.5-6 nm thick with the critical temperature of about 11-12 K. For these devices we achieved the receiver noise temperature $T_R(\text{DSB})=3000$ K in the 500-700 GHz frequency range and an IF bandwidth of 3-4 GHz. Preliminary measurements at frequencies 1-1.2 THz resulted the receiver noise temperature about 9000 K (DSB).

1. Introduction

Superconducting hot electron bolometric (HEB) mixers are a promising technology for the Terahertz frequencies since this technology can be extended to frequencies of tens of THz due to the physical mechanism employed and the small parasitic reactance. For the phonon cooled HEB mixer based on thin NbN films, the technology level of the films achieved so far allows one to predict the minimum noise temperature of ~ 100 K (plus the quantum noise) [1]. For this reason, one can expect lower values for this temperature as compared to SIS mixers for frequencies greater than ~ 700 GHz. However, the noise temperature values obtained for the waveguide version of the HEB mixer amount to 500 K for 100 GHz [2], 750K for 244 GHz [3] and 650K for 533 GHz [4]. For the

quasioptical version, which is promising for higher frequencies, only preliminary results have been reported [5,6].

Achieving a broad intermediate frequency bandwidth has always been a major difficulty for the bolometer mixers. The maximum bandwidth calculated from the electron-phonon relaxation time at T_c , $\tau_{eph}(T_c)$, reaches ~ 10 GHz [7] for phonon cooled HEB mixers based on NbN thin films. For the diffusion cooling mechanism it is only limited by the possibility to reduce the distance between the contacts by lithography and can well be of the same order of magnitude, although the previously reported IF bandwidth values for both HEB mixer types amount to 1,5-2 GHz [2,4]. Only at this symposium has a wider IF bandwidth been reported: 4 GHz for the phonon cooled NbN HEB at the frequency of 140 GHz [8] and 6 GHz for the diffusion cooled Nb HEB at the frequency of 20 GHz [9]. For the first type of mixers, in order to expand the frequency bandwidth one has to employ very thin films with a high superconducting transition temperature, which leads to a disproportional growth of the sheet resistance of the film and complicates its coupling with the planar antenna. In this paper we report the results of an experimental study of a spiral antenna-coupled, phonon-cooled NbN HEB and noise temperature measurements in the 0,5-1,2 THz frequency range as well as the intermediate frequency bandwidth. For these devices we achieved the receiver noise temperature $T_R(\text{DSB})=3000$ K in the 500-700 GHz range and an IF bandwidth of 3-4 GHz. In preliminary measurements at the frequencies of 1-1.2 THz, T_R reached about 9000 K.

2. Device fabrication.

30-50 A thick NbN films were sputtered on sapphire and silicon substrates by magnetron reactive sputtering in an argon-nitrogen mixture. The film geometry was shaped by photolithography to produce a single strip or several parallel strips connected to an antenna fabricated from a Ti-Au layer. A more detailed description of the NbN thin film fabrication can be found in [8]. Parameters of mixer chips are presented in Table 1.

Table 1
Specification for the devices

#	Substrate	Thickness [Å]	R_{15K} [kΩ]	T_c [K]	ΔT_c [K]	$I_c(4.5K)$ [mA]
1	sapphire	35	0.15	11	0.7	0.55
2	Si	50	0.25	11.6	0.5	1.3
3	Si onsap	60	0.20	12.5	0.3	1.5
4	Si	50	0.35	11	0.6	0.75

Fig. 1a is a photo of a spiral antenna-coupled NbN HEB mixer. Figs. 1b,c,d show the central part of these mixers for several options of the NbN film geometry. For 50 Å thick films, one, two, three or four parallel strips 1-2 μm long by 1 μm wide (Fig.1d) were connected to the antenna. Thus allows one to vary the mixer normal state resistance R_n . This resistance for high radiation frequencies, when the quantum energy is much higher than the energy gap, coincides with the RF impedance of the device. However, for lower frequencies, which are also used in this work, this impedance is lower than R_n and is difficult to estimate. Its matching with the antenna can only be achieved experimentally, i.e. by varying the number of parallel strips.

For thinner NbN films (35 Å thick), the geometry of Fig.1d leads to far greater R_n than the antenna impedance, and the mixer element does not match the antenna impedance. For better coupling, it would be necessary to reduce the length of the strips, that is to

reduce the gap in the antenna slot into which the NbN strips are inserted. This entails a reproduction of submicron dimensions and a shift to electron lithography, which makes manufacturing of the mixer chips much more expensive. Since during this work many dozens of mixer chips have been manufactured, this factor would be important. Another way, which consists in increasing the number of parallel strips is unacceptable since it entails a lengthening of the antenna slot, which occupies the central area of the antenna and for that reasons restricts the upper limit of the antenna frequency. Due to this fact we have developed another two structure geometries. The first geometry has no gaps between the strips, so that it is a single wide ($6\ \mu\text{m}$) and short ($1\text{-}1.5\ \mu\text{m}$) strip made of ultrathin NbN film (Fig. 1b). This film is so thin and so transparent that it is hardly possible to see or photograph it. For this reason the picture only shows the antenna slot. A relatively large width of the strip ($6\ \mu\text{m}$) together with a great length would lead to an extra roll-off IF signal at low frequencies because of the return flow of nonequilibrium phonons from the substrate into the film, but small length ($1\ \mu\text{m}$) makes the film geometry for the phonons equivalent to a narrow strip.

The choice of the film geometry shown in Fig.1b allows one to make R_n twice as low as compared to the geometry in Fig.1d with the same dimensions of the antenna slot.

However, it can prove insufficient if ultrathin NbN films with a sheet resistance of $\sim 800\ \text{Ohm/sq}$ and more are used with an antenna with impedance of $70\ \text{Ohm}$. The third geometry (Fig.1c) makes it possible to use the central area even more effectively and, as a matter of fact, to make R_n three times lower with the same linear dimensions of the slot: three gaps are here inscribed into a $6\ \text{by}\ 6\ \mu\text{m}^2$ square and connected in parallel to the DC bias and the RF. Here we have left three parallel strips $1\ \mu\text{m}$ wide (because of

the small thickness of the NbN film, they cannot be seen on the photo either). Further progress in this direction will apparently require the use of electron lithography.

3. Experiment and discussion.

The mixer block with a spiral antenna coupled NbN HEB mixer was mounted in a LHe cooled vacuum cryostat that was equipped with SMA connectors for the IF signal and DC-bias. The LO and signal radiation were fed through a Teflon window and a black polyethylene filter on the IR-radiation shield to a planar spiral antenna behind an extended hemispherical Si lens with anti-reflection coating. A resistive heater and a thermometer were attached to the mixer mount to control the temperature. The radiation of the local oscillator LO was focused by a Teflon lens and combined with the signal through a 50 μm thick Mylar beam splitter.

Three backward wave oscillators (BWOs), partially overlapping in frequency, were used as Los in the 0.5-1.25 THz range. The power of each of them was sufficient to pump the mixers almost to their normal state even after the loss in the beam splitter and optics.

The bandwidth of the mixer was measured using two identical BWOs for 520-720 GHz operation. One of them was used as the local oscillator and the other one as the signal source. The frequency of the second one was fixed (e.g. at 660 GHz), whereas the first one was tuned in such a way that the IF varied from 0 to 7 GHz. The LO power was adjusted in every point and remained optimal for the conversion gain. The IF signal was measured by a spectrum analyzer after amplification by two room temperature 0.1-20 GHz amplifiers.

For noise measurements, a cooled 680-900 MHz low noise IF amplifier with a noise temperature about 6.5 K and a bias-T were added to the IF line inside the cryostat. The output frequency was converted down to 0-100 MHz band and detected by a scalar network analyzer.

Fig. 2 shows the unpumped IV-curves for device No. 2 at 4.5 K, 10.5 K and 11 K, and the IV-curve when the device was pumped by a 660 GHz LO at 4.5 K. On each IV-curve one can see the superconducting state region with some series resistance due to the contacts. On two of the curves one can observe a region where instabilities occur after the current exceeds its critical value. This region is presented as a straight line, although this part of the IV-curve could not be recorded using a DC bias scheme. When the pumped IV-curve is compared with the unpumped one for 10.5 K and 11 K, it is apparent that the former is clearly nonthermal, and that it intersects the two thermal curves in two points each. This testifies to the fact that the quantum energy for radiation of 660 GHz frequency is substantially less than the energy gap for this NbN film. At the same time, the IV-curve pumped by optimum LO power (Fig.3) for the frequency of 1 THz is very close to the pumped one at $T=8.8$ K, since the quantum energy here already exceeds the energy gap.

For mixer chip No. 1, made of NbN film 35 Å thick, the value of the energy gap is less than that of mixer chip No. 2, and for both frequencies (660 GHz and 1 THz) the pumped IV curves are close to each other and to the unpumped one at 10 K (Fig. 4). A comparison between the noise temperature and the IF bandwidth for HEB devices made of NbN films 50 Å thick and 35 Å thick shows that the latter yield better results for the frequency of 660 GHz in both measures. Fig. 5 shows the output signal vs. intermediate

frequency for mixer chip No. 1 and at two working temperatures for mixer chips No. 2. As the temperature increases, the bandwidth of the mixer widens from 800 MHz at $T=4.5$ K up to 2 GHz at 12.3 K, whereas the noise temperature shows a considerable growth. The increase of the bandwidth with the temperature allows one to conclude that under optimal LO power at $T_a=4.5$ K the electron temperature is far from reaching T_c and that the bandwidth is limited by the heating processes at the boundary between the NbN film and the substrate. For a thinner film (mixer chip No. 1), the IF bandwidth is significantly wider even at an ambient temperature of 4.5 K and amounts to 3.5 GHz (Fig.5). Such a wide bandwidth, as well as the agreement of the pumped IV curve with the unpumped one at $T=10$ K, can be viewed as evidence of the fact that this mixer operates in the pure hot electron mode and that the electron temperature at the optimal point reaches 10 K.

The results of the noise temperature measurements are shown in Fig. 6. The best results regarding noise were obtained for mixer chip No. 1. This figure presents data on the noise temperature in the frequency range of 520-700 GHz. The value of T_R varies from 2800 K to 3200 K for these frequencies.

The noise temperature measurements in the frequency range of 1÷1.2 THz for mixer chip No. 1 yielded values of $T_R \approx 9000$ K, i.e. substantially higher than in the 520-700 GHz. Since the pumped IV-curves almost coincide here, it can be concluded that the reason for this is worsening of the coupling factor with growing frequency. We are working to improve our measuring setup and optics for accurate measurements at above 1 THz frequency range.

4. Calculation of IV-curves

To predict the performance of a HEB mixer one needs to know the behaviour of DC IV-characteristics. They can be derived from the relation between the bolometer resistance and temperature, $R(T)$ and dR/dT . The calculations are based on Eqs. 1 and 2, which are obtained from the heat balance equation, Eq. 3.

$$C = I^2 \frac{dR}{d\Theta} \cdot \frac{\tau_{eph}}{C_e} \quad (1)$$

$$\frac{dV}{dI} = R(\Theta) \frac{1+C}{1-C} \quad (2)$$

$$C_e \frac{d\Theta}{dt} = -\Pi(\Theta, T) + P_{DC} + P_{RF} \quad (3)$$

τ_{eph} is the electron-phonon relaxation time, C_e is the heat capacity of the electron system, Θ is the electron temperature, Π is the heat flow from the electron system to the phonon system, P_{DC} and P_{RF} are the absorbed DC and RF power. The use of these equations is valid only for uniform heating of the HEB by radiation and DC power, i.e. for signal frequencies corresponding to energies larger than the energy gap of the thin superconducting film. Moreover, the expression for the self-heating parameter is only valid for equivalent electron temperatures close to T_c . We have assumed that only a part of the volume of the device is taken into account for the bolometer heat capacity. This part increases with the DC resistance of the device and can be viewed as the volume of a normal domain or similar non superconducting region of the bolometer strip. The electron-phonon relaxation time and the heat capacity in Eq. 1 have the temperature dependencies $\Theta^{-1.6}$ and Θ respectively.

The calculation of the IV-characteristic is made in steps along the curve and starts at a point very close to zero voltage and current at an equivalent electron temperature given by the ambient temperature. The subsequent points on the IV-curve are reached by increasing the voltage in small steps and applying the differential resistance obtained by Eqs. 1 and 2. For each point on the IV-curve the DC resistance gives the equivalent electron temperature Θ and $dR/d\Theta$, which are used to derive the differential resistance leading to the next point.

Fig. 7 shows the measured resistance and $dR/d\Theta$ vs. temperature for mixer chip No.2. The calculated IV-curves for two different ambient temperatures (11.2 and 11.4K) as well as two measured IV-curves are shown in Fig. 8. The shape of the calculated and measured IV-curves agree reasonably well. The method to calculate the IV-curve is under development and will be improved to allow ambient temperatures far below T_c , and make it possible to estimate the mixer conversion gain for low physical temperature and large pump power. The correspondence between the measured and calculated curves can be viewed as an indication on how well the present theory for superconducting HEB mixers works.

5. Acknowledgments

This work has been supported by the European Space Agency (Contract AOP/WK/330038), Swedish National Space Board (Contract Dm. 22/95), and Russian Program on Condensed Matter (Superconductivity Division) under Grant No. 93169.

6. References

1. B.Karasik, and A.Elantev. "Analysis of the Noise Performance of a Hot-Electron Superconducting Bolometer Mixer." Proc. of the 6th Int. Symp. on Space Terahertz Tech., Caltech, Pasadena, pp.229-246, 1995.
2. O.Okunev, A.Dzardanov, G.Gol'tsman, and E.Gershenson. "Performances of Hot-Electron Superconducting Mixer for Frequencies Less than the Gap Energy: NbN Mixer for 100 GHz Operation." Proc. of the 6th Int. Symp. on Space Terahertz Tech., Caltech, Pasadena, pp.247-253, 1995.
3. J.Kawamura, R.Blundell, C.-Y.E.Tong, G.Gol'tsman, E.Gershenson, and B.Voronov. "Superconductive NbN Hot-Electron Bolometric Mixer Performance at 250 GHz", This conference proceedings.
4. A.Scalare, W.McGrath, B.Bumble, H.LeDuc, P.Burke, A.Vereijen, and D.Prober. "Noise Temperature and IF Bandwidth of 530 GHz Diffusion-cooled Hot-electron Bolometer Mixer." Proc. of the 6th Int. Symp. on Space Terahertz Tech., Caltech, Pasadena, pp.262-267, 1995.
5. H. Ekstrom, B. Karasik, E. Kollberg, G. Gol'tsman, and E. Gershenson. "350 GHz NbN Hot Electron Bolometer Mixer." Proc. of the 6th Int. Symp. on Space Terahertz Tech., Caltech, Pasadena, pp.269-283, 1995.
6. E. Gerecht, C.F. Musante, C.R. Lutz, Z. Wang, J. Bergendahl, K.S. Yngvesson, E.R. Mueller, J. Waldman, G.N. Gol'tsman, B.M. Voronov, and E.M. Gershenson, presented at the Intern. Semicond. Device Res. Symp., Charlottesville, VA , pp.619-622, 1995.
7. Yu.P.Gousev, G.N Gol'tsman, A.D. Semenov, E.M. Gershenson, R.S. Nebosis, M.A. Heusinger, and K.F. Renk. "Broadband Ultrafast Superconducting NbN Detector for Electromagnetic Radiation." J. Appl. Phys., vol.75, No 7, pp.3695-3697, 1994.
8. P. Yagoubov, G. Gol'tsman, B. Voronov, L. Seidman, V. Siomash, S. Cherednichenko, and E. Gershenson. "The Bandwidth of HEB Mixers Employing Ultrathin NbN films on Sapphire Substrate", This conference proceedings.
9. R.Schoelkopf, P.Burke, D.Prober, A.Scalare, W.McGrath, B.Bumble, and H.LeDuc. "Large Bandwidth Mixing in Diffusion-Cooled Hot-Electron Microbolometers", This conference proceedings.

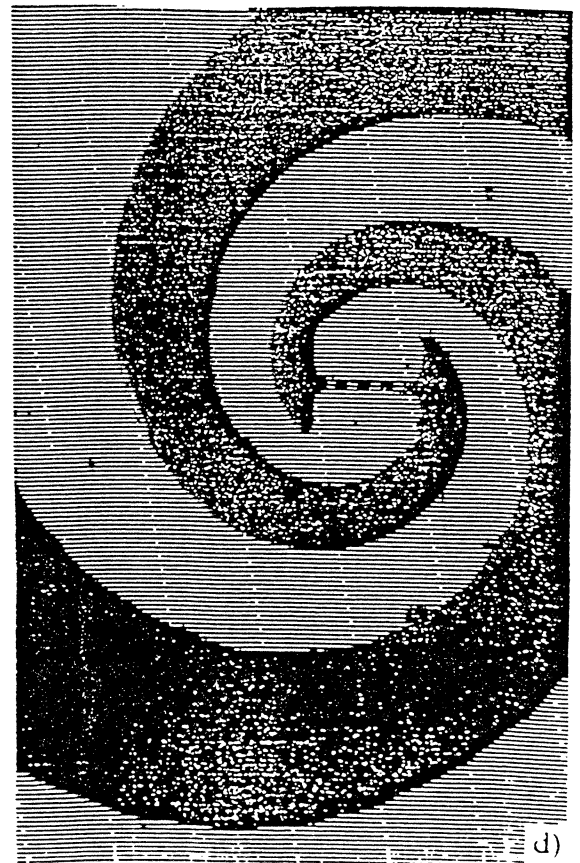
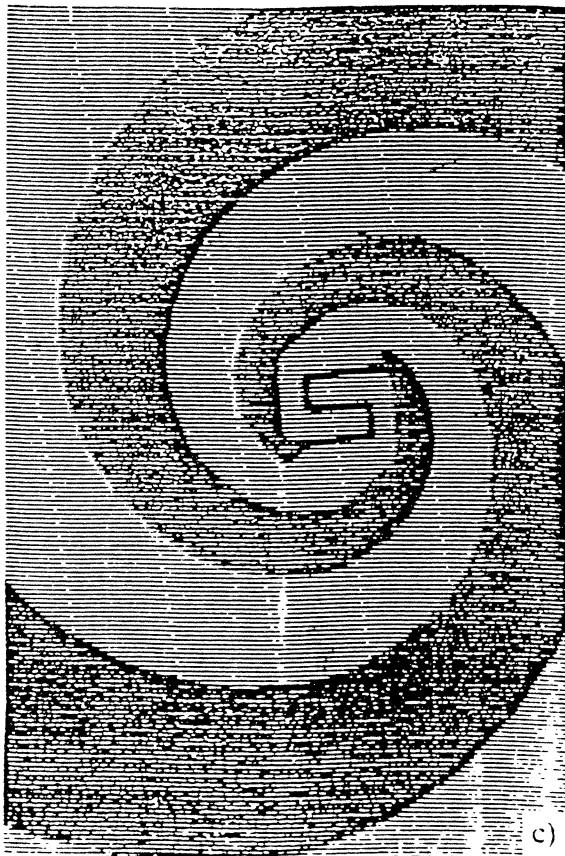
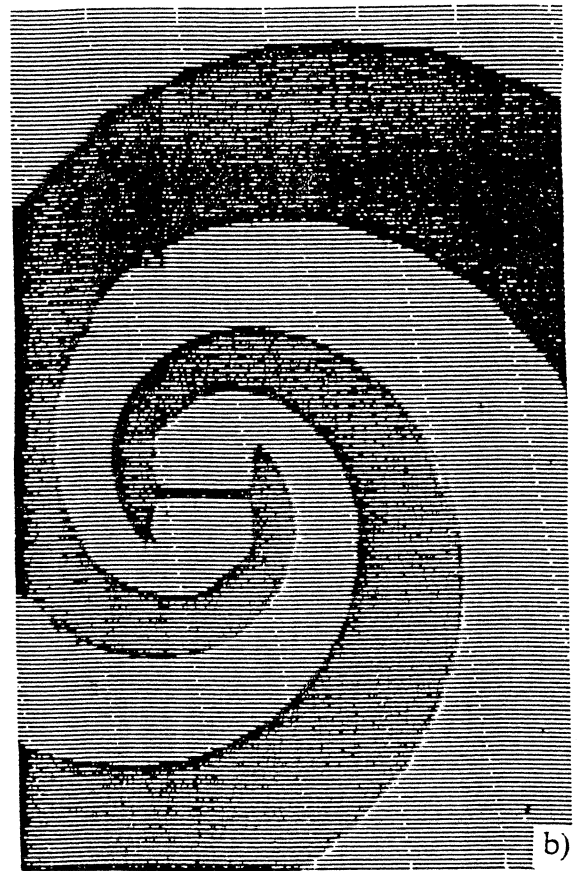
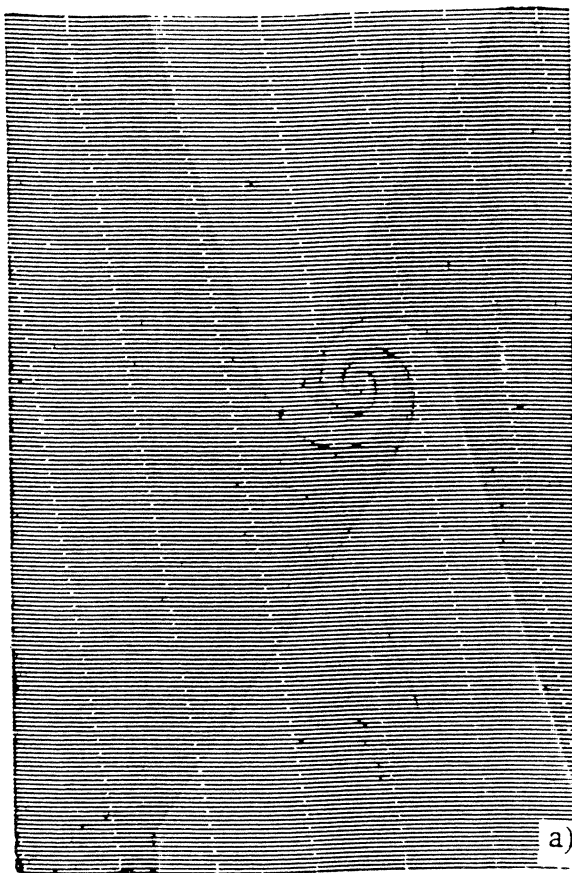


Figure 1

a) Photo of a spiral antenna coupled NbN HEB mixer

b), c), d) show the central part of these mixers for several variants of NbN film geometry

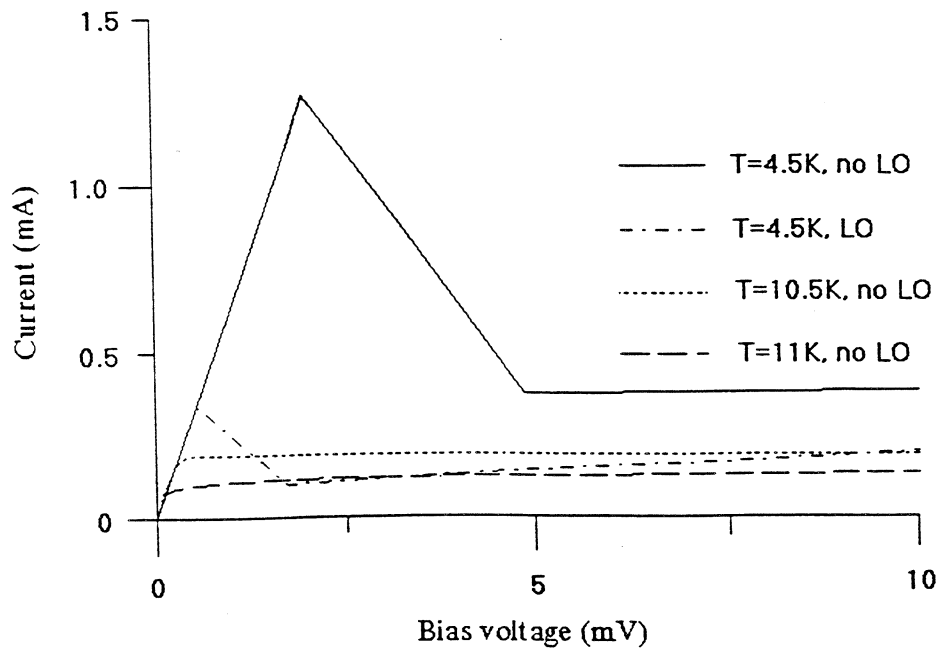


Figure 2
Pumped by 660 GHz and unpumped IV-curves for mixer chip #2 at different temperatures

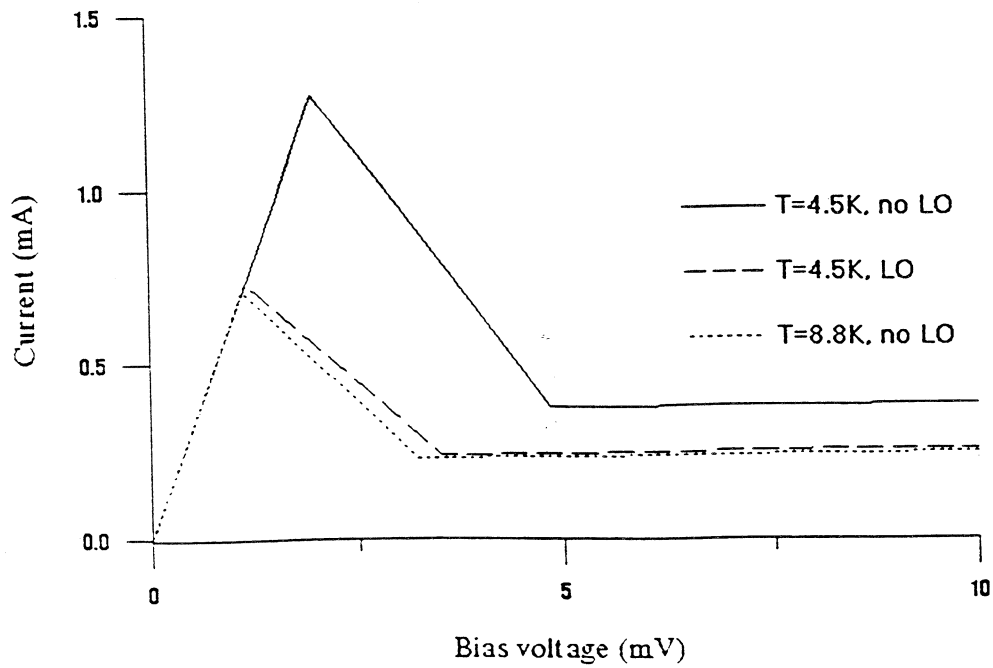


Figure 3
Pumped by 1 THz and unpumped IV-curves for mixer chip #2 at different temperatures

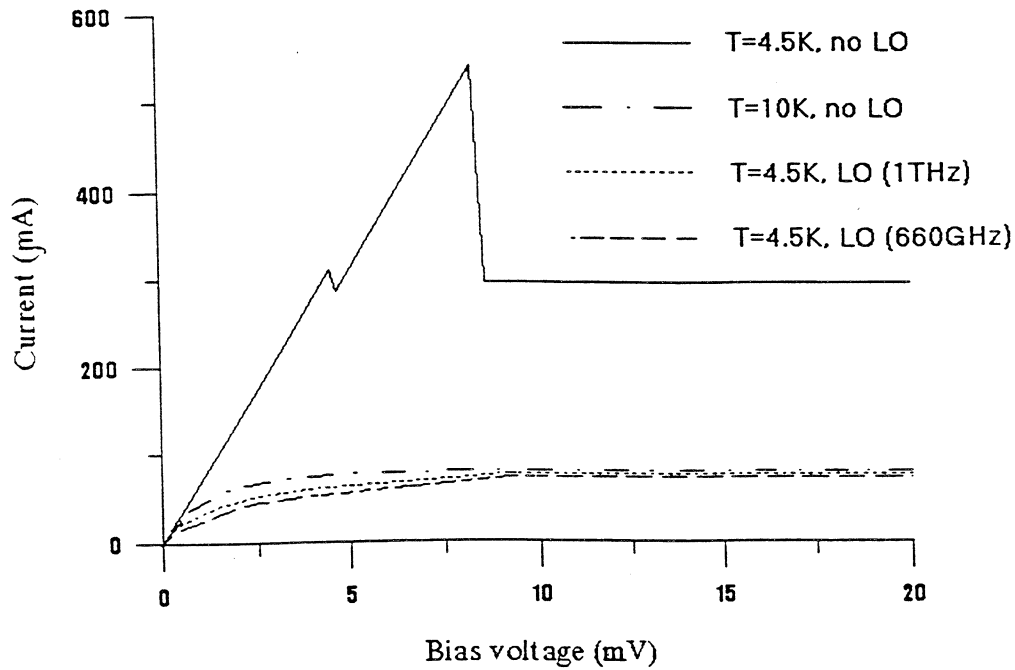


Figure 4
Pumped by 660 GHz or 1 THz IV-curves for mixer chip #1 at different temperatures

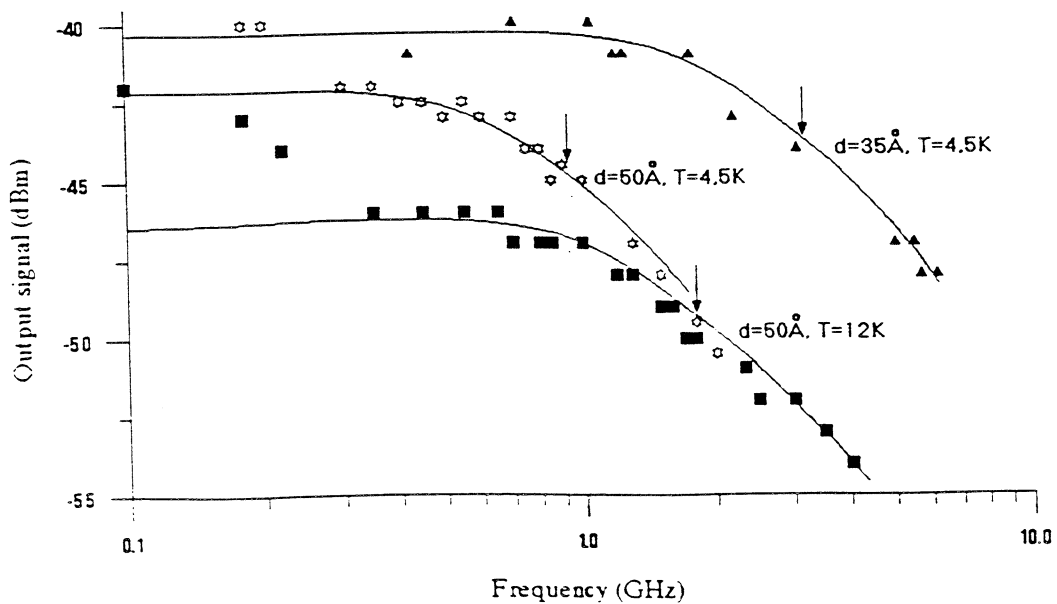


Figure 5
Output signal for NbN HEB mixer chips (#1 and #2) vs. Intermediate frequency at different ambient temperatures

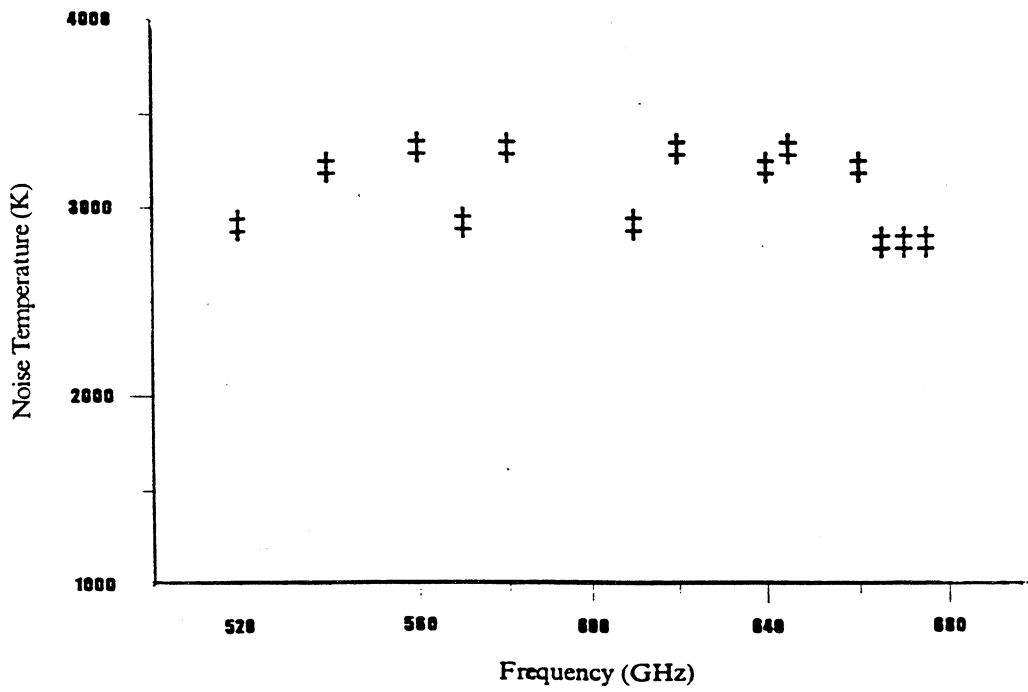


Figure 6
Frequency dependence of DSB noise temperature for device # 1

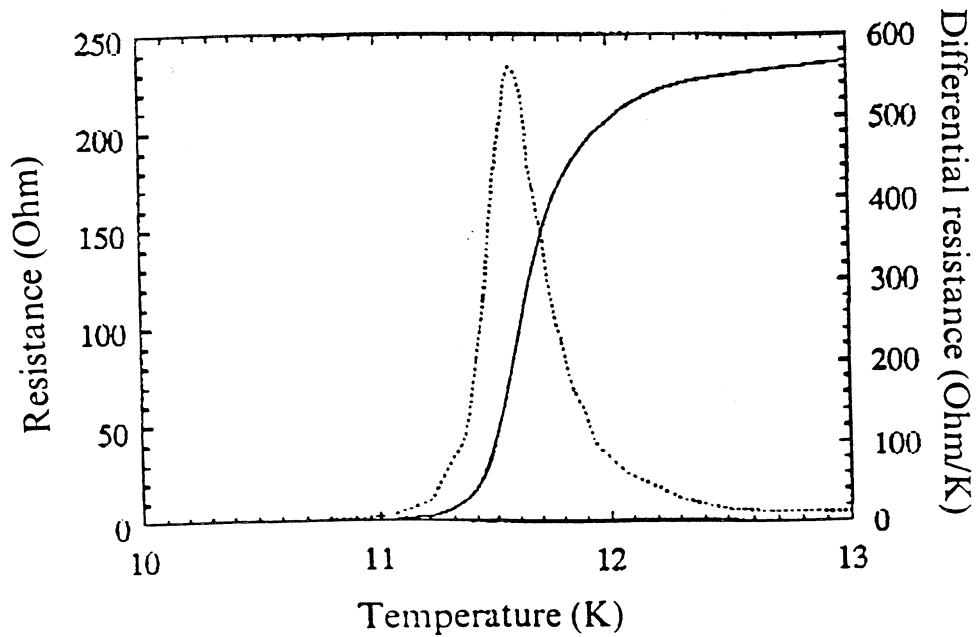


Figure 7
Measured resistance vs temperature

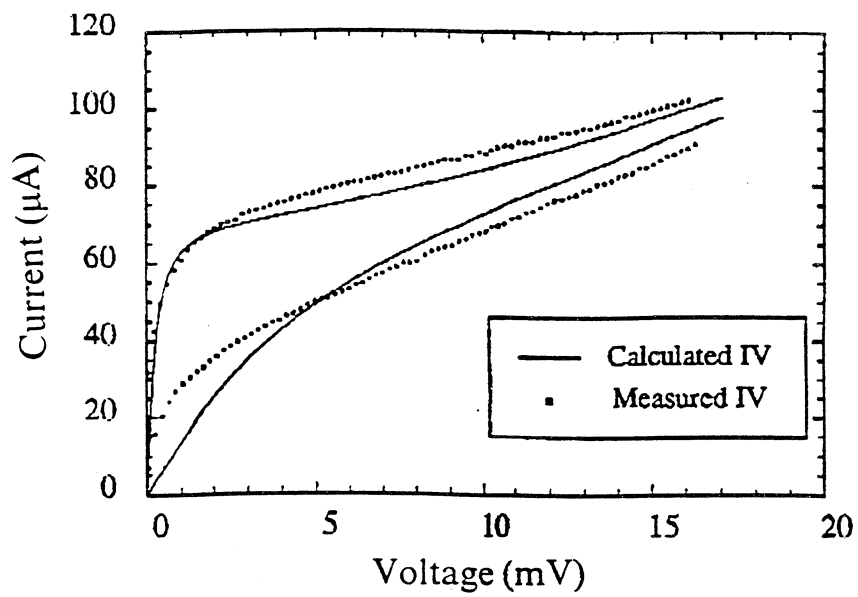


Figure 8
Calculated and measured IV-characteristics